Journal of Thermal Analysis and Calorimetry, Vol. 65 (2001) 221–229

THERMAL BEHAVIOR OF Cu–Al ALLOYS NEAR THE α-Cu–Al SOLUBILITY LIMIT

A. T. Adorno, M. R. Guerreiro and A. V. Benedetti

Departamento de Físico-Química, Instituto de Química – UNESP, Caixa Postal 355, 14801-970 Araraquara, SP, Brazil

(Received January 17, 2000; in revised form February 20, 2001)

Abstract

The thermal behavior of Cu–Al alloys with 17, 19 and 21 at.%Al was examined by differential thermal analysis (DTA), differential scanning calorimetry (DSC), X-ray diffractometry (XRD), optical microscopy (OM) and scanning electron microscopy (SEM). The presence of the gamma phase (Al_4Cu_9) was clearly detected for the Cu–19 at.%Al alloy and caused the α_2 phase disordering process in two stages. The tendency to increase the α_2 dissolution precipitates with the increase in the Al content seems to be reverted for compositions at about 21 at.%Al and the heating/cooling ratio seems to influence the thermal response of this process. The presence of the endothermic peak corresponding to the $\beta_1 \rightarrow \beta$ transformation depends on an incomplete β decomposition reaction. The variation of the heating rate showed that the $\beta_1 \rightarrow (\alpha+\gamma_1)$ decomposition is the dominant reaction for alloys containing 19 and 21 at.%Al.

Keywords: Cu–Al system, differential scanning calorimetry, stable and metastable phase transformations

Introduction

The order-disorder phenomena in copper-rich Cu–Al alloys present interesting features concerning the ordered equilibrium α_2 phase and the disordered high temperature β phase [1, 2]. According to Murray [3], the solubility of Al in (Cu) is 19.7 at.%Al at the eutectoid temperature (567°C) and less than 17 at.%Al between 400°C and room temperature. The (Cu)/((Cu)+γ_1) boundary is vertical between the eutectoid temperature and 400°C. A two-phase (Cu)+β field exists between the eutectic temperature and the eutectoid reaction $\beta \rightarrow \gamma_1$+(Cu). West and Thomas [4] discovered the phase α_2 in equilibrium with (Cu) and γ_1 below a peritectoid reaction (Cu)+$\gamma_1 \rightarrow \alpha_2$, by prolonged annealing experiments carried out at temperatures in the range 340–400°C on binary copper–aluminum alloys containing 0.7 to 16.5 mass%Al. On the other hand, for Al concentrations exceeding the solubility limit of α-Cu–Al Gaudig and Warlimont [5], studying the structure of short range ordered α-Cu–Al alloys, found two different superlattice phases, α_2 and α_3.

1418–2874/2001/ $ 5.00

Akadémiai Kiadó, Budapest
Kluwer Academic Publishers, Dordrecht

Kwarciak [6] studied the phase transformations in Cu–12.4 mass%Al and Cu–14.4 mass%Zn–8.4 mass%Al by DTA and found that the rates of heating and cooling were the major factors determining the transformations which take place in these alloys. Kwarciak *et al.* [7] studied the phase transformation in martensite of Cu–12.4%Al by DTA and determined the influence of the heating rate on the phase transformation.

Two aspects from the available literature about the phase transformations in copper-rich Cu–Al alloys call for attention: a) the $\gamma_1/(\gamma_1+(Cu))$ boundary is accurately delineated and the placement of the (Cu) solvus is uncertain [3] and b) depending on the heat treatment the published $\beta/\beta+\beta_1$ limit may be shifted for low compositions [2]. In order to get more information, three Cu–Al alloys with 17, 19 and 21 at.%Al were used to examine the influence of the presence of the γ_1 (Al_4Cu_9) phase on the thermal behavior of these alloys, using DTA, DSC, XRD, OM and SEM.

Experimental procedure

Three Cu–Al alloys were prepared in an induction furnace under argon atmosphere, using a graphite crucible and Cu 99.99% and Al 99.99% as starting materials. The compositions of the alloys were chemically analyzed to be 17.0, 19.0 and 21.0±0.5 at.%Al, using a VARIAN Intralab AA-1475 atomic absorption spectrophotometer.

Cylindrical samples with 2.0 cm diameter and 6.0 cm length were cut in disks of 0.4 cm thickness and small square pieces of about 3.0 mm length were used for DTA and DSC analysis. The disks were cold rolled for optical and scanning electron microscopy. The samples were annealed during 120 h at 850°C for homogenization. After annealing, some of them were equilibrated at 850°C for 1 h and then quenched in iced water.

DTA data were obtained using a TA SDT 2960 and DSC data were obtained using a TA 2910 instrument. After the heat treatments, the samples were polished, etched and examined by optical microscopy (OM) using a Carl Zeiss Neophot 30 and by scanning electron microscopy (SEM) using a Jeol JSM T330A. The XRD diagrams were obtained using a HZG-4B X-ray diffractometer and solid (not powdered) samples.

Results and discussions

Figure 1 shows the DTA curves obtained for the Cu–17 at.%Al (Fig. 1a), Cu–19 at.%Al (Fig. 1b) and Cu–21 at.%Al (Fig. 1c) alloys and it is possible to observe that curves in Fig. 1b and c show an endothermic peak at about 570°C while Fig. 1a presents only a poorly defined peak at about 550°C. This peak is due to the $(Cu)+\gamma_1 \rightarrow \beta$ eutectoid transformation, as expected from the Cu–Al equilibrium diagram [8]. The peak in Fig. 1a indicates that the Al content in the Cu–17 at.%Al alloy is not enough for the formation of a significative quantity of the γ_1 phase.

In order to get more information about the phase transformations in these alloys the DSC, a more sensitive technique, was used.

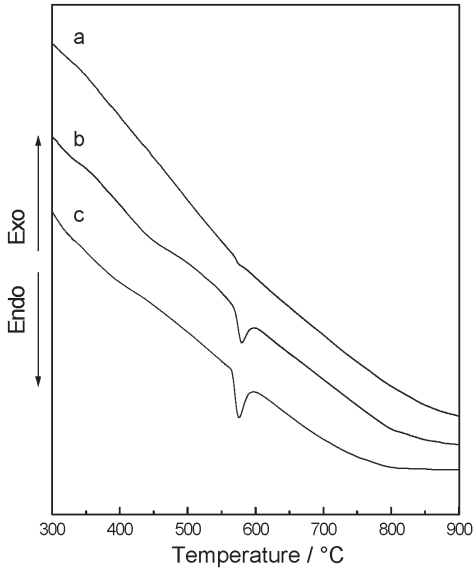

Fig. 1 DTA curves for the annealed alloys: a – Cu–17 at.%Al; b – Cu–19 at.%Al; c – Cu–21 at.%Al

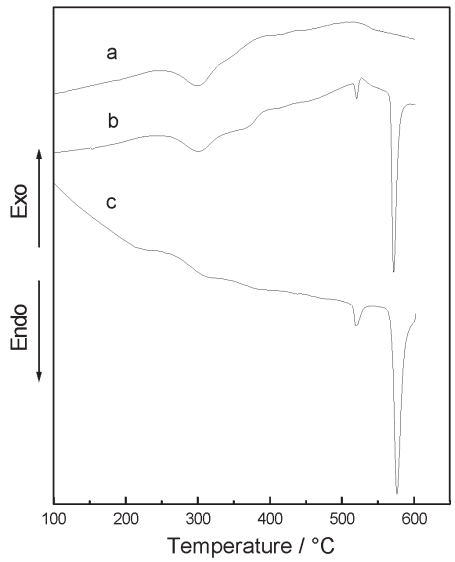

Fig. 2 DSC curves for annealed samples: a – Cu–17 at.%Al alloy; b – Cu–19 at.%Al alloy, c – Cu–21 at.%Al alloy. Alloys cooled at about 4°C min^{-1} before heating at 20°C min^{-1}

Figure 2 shows the DSC curves obtained for the Cu–17 at.%Al (Fig. 2a), Cu–19 at.%Al (Fig. 2b) and Cu–21 at.%Al (Fig. 2c) alloys at a heating rate of 20°C min^{-1} for

annealed samples. All curves show an endothermic peak at about 300°C which corresponds to the order-disorder transition (Cu)-α+α_2→(Cu)-α+(α+γ_1), i.e., this peak is associated with disordering the α_2 phase [6]. The presence of an endothermic peak at about 200°C in the curve of Fig. 2c may indicate that this disordering process occurs in two stages. Figure 2b shows, in addition, three endothermic peaks at about 380, 520 and 570°C and the peak at 380°C is not clearly observed in the curve of Fig. 2c.

The peak at 380°C is due to the dissolution of α_2 precipitates formed during slow cooling [9]. This peak was also observed for alloys with Al concentrations of 19 and 19.5 at.% and it is increased at 19.5 at.%Al [5]. This result could indicate an increase in the peak intensity for Al concentrations higher than 19.5 at.%. However, the peak at 380°C is not well defined for the alloy with 21 at.%Al, indicating a strong decrease in the dissolution of α_2 precipitates. This may be explained considering that the fraction of the α-matrix phase in the alloys exceeding the solubility limit of α-Cu–Al is decreased with the increase of the Al content, leading to a decrease in the dissolution of α_2 precipitates in the matrix. The endothermic peak at 520°C is associated with transformation of the β_1 phase into β. The martensite β_1' changes into the β_1 phase in the same temperature interval as the disordering process of the α_2 phase and at about 520°C the β_1 phase transforms into the β phase [6]. The peak at 570°C is due to the (Cu)-α+(α+γ_1)→(Cu)-α+β transformation [3]. All the results obtained are according to the literature about the stable copper-rich phases transformations. They also indicate that at the composition of 17 at.%Al it is not possible to detect the presence of the gamma phase by the techniques here employed. As shown in Fig. 3, this alloy presents only the structure and the diffraction lines characteristic of the α phase. In addition, the results indicate a reversion on the tendency to increase the dissolution of α_2 precipitates with the increase of Al concentration.

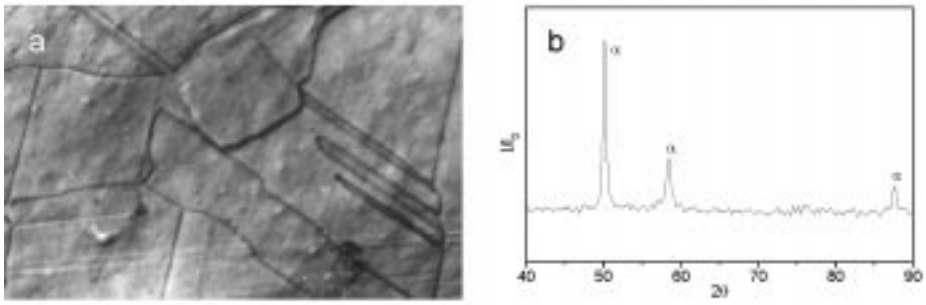

Fig. 3 Cu–17 at.%Al alloy after annealing: a – optical micrograph (350×); b – X-ray diffraction pattern

It is known that the heating rate is determinant in the observation of the peak at 520°C [6]. Figure 4 shows the DSC curves obtained for the Cu–19 at.%Al alloy using annealed samples. Curve labeled a was obtained in the same conditions as curve b shown in Fig. 2, i.e., cooling at about 4°C min^{-1} before heating at 20°C min^{-1}. Curve labeled b in Fig. 4 was obtained cooling the alloy at 1°C min^{-1} and then heating at 20°C min^{-1}. It is

possible to observe that the endothermic peak at 520°C, corresponding to the $\beta_1 \rightarrow \beta$ phase transformation is not present in curve b. Kwarciak [6] observed that this endothermic peak was detected in samples cooled, before heating, at a rate of 10°C min^{-1} and not detected for samples cooled at 2°C min^{-1}. Therefore, for samples cooled at a rate equal or lower than 2°C min^{-1}, during reheating only two endothermic effects were observed, the disordering of the α_2 phase and the (Cu)-α+(α+γ_1) $\rightarrow$ (Cu)-α+β transformation. The presence of the endothermic peak at about 520°C depends on an incomplete (Cu)-α+β $\rightarrow$ (Cu)-α+(α+γ_1) transformation, which retains a small fraction of the martensitic phase. This retained martensite changes into the β_1-phase in the same temperature interval as the second stage of α_2 disordering process. At about 520°C the $\beta_1 \rightarrow \beta$ phase transformation occurs. Therefore, for cooling rate in which the martensitic phase is not retained, e.g. 1°C min^{-1}, the endothermic peak at about 520°C was not observed.

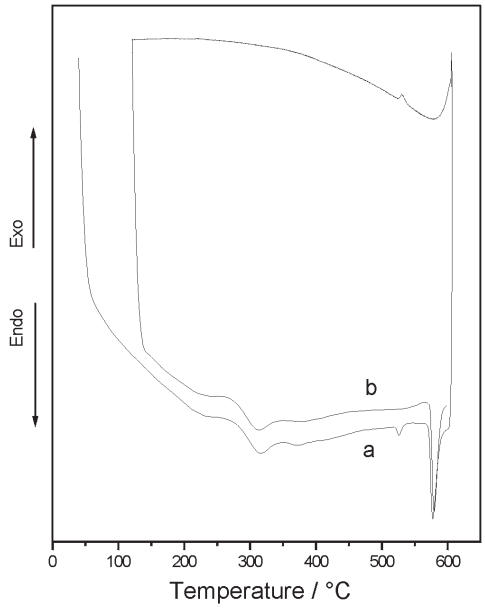

Fig. 4 DSC curves obtained for the Cu–19 at.%Al alloy: a – cooled at about 4°C min^{-1} before heating at 20°C min^{-1}; b – cooling at 1°C min^{-1} and then heating at 20°C min^{-1}

It can be seen in Fig. 4 that in the heating curve the peak at about 300°C is well defined but in the cooling curve the corresponding peak is not detected. According to Kwarciak [6], for a Cu–12.4 mass%Al alloy an exothermic peak at about 300°C ascribed to the $\alpha \rightarrow \alpha_2$ transition is observed at a cooling rate of 10°C min^{-1}, which presents a very low intensity at a cooling rate of 2°C min^{-1}. As expected this exothermic peak is not observed for a cooling rate of 1°C min^{-1}.

Figure 5 shows the enlarged portion of Fig. 4 corresponding to the region for α_2 phase disordering and precipitates dissolution. It is interesting to notice that the endo-

thermic peak at 380°C is better defined in Fig. 5a, obtained for the sample cooled at about 4°C min^{-1} and reheated at 20°C min^{-1}, than in Fig. 5b, corresponding to the sample cooled at 1°C min^{-1} and reheated at 20°C min^{-1}. And both of them are better

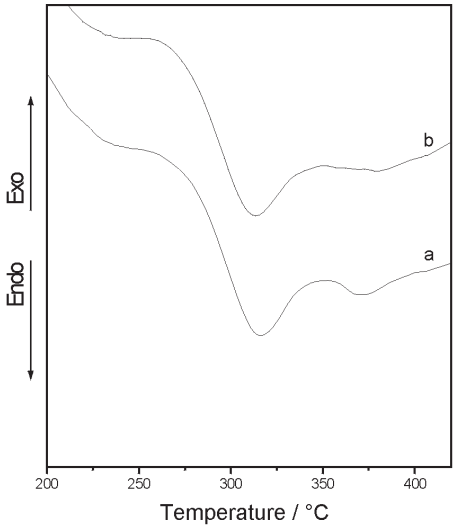

Fig. 5 Enlarged part of Fig. 4, showing the region for α_2 disordering and precipitates dissolution

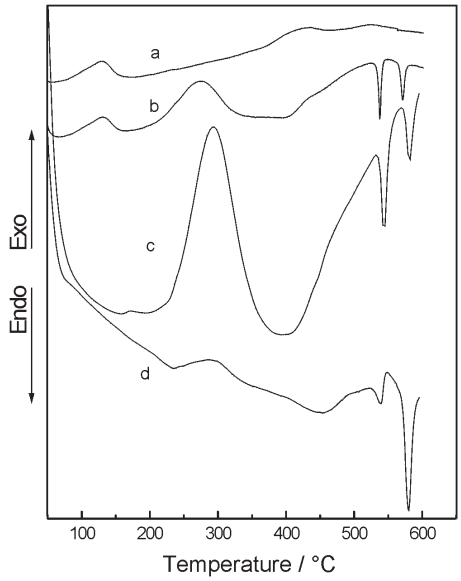

Fig. 6 DSC curves obtained for alloys quenched before heating at 20°C min^{-1}: a – Cu–17 at.%Al; b – Cu–19 at.%Al; c – Cu–21 at.%Al; d – Cu–21 at.%Al quenched before heating at 30°C min^{-1}

defined than the peak observed for the same alloy cooled at 5°C h^{-1} and reheated at 5°C min^{-1} [5]. This may indicate a relationship between the heating/cooling ratio and the peak definition. The three cited ratios are 5, 20 and about 60, respectively and the lower ratios give well-defined peaks. Considering that the order-disorder process is a reversible one, when the heating/cooling ratio increases a thermal response far away from reversibility is expected. In this way, smaller heating/cooling ratio could better define the peak observed at 380°C.

Figure 6 shows the DSC curves obtained for the Cu–17 at.%Al (Fig. 6a), Cu–19 at.%Al (Fig. 6b) and Cu–21 at.%Al (Fig. 6c) alloys quenched from 850°C in iced water before heating at 20°C min^{-1}. It also shows the DSC curve obtained for the Cu–21 at.%Al alloy quenched before heating at 30°C min^{-1} (Fig. 6d). Curves in Fig. 6a and b show an exothermic peak at about 130°C and in Fig. 6c at about 170°C. This peak may be ascribed to the first stage of the ordering of α_2 phase. Curves in Fig. 6b and c show another exothermic peak at about 270°C. This second peak is due to the ordering of the β' martensitic phase ($\beta' \rightarrow \beta'_1$). These curves also show three endothermic peaks, at about 400, 535 and 570°C. The peak at 400°C is asymmetrical and is associated to the reverse martensitic transformation $\beta'_1 \rightarrow \beta'$ and the decomposition $\beta_1 \rightarrow (\alpha+\gamma_1)$ from part of the β_1 phase. The peak at 535°C is related to the transition $\beta_1 \rightarrow \beta$ from the remaining part of the β_1 phase formed at 400°C and the peak at 570°C is due to the $(\alpha+\gamma_1) \rightarrow \beta$ transformation [7].

It is observed that the first exothermic peak decreases with the increase of the Al content and is shifted to a higher temperature for the Cu–21 at.%Al alloy. Popplewell and Crane [10] observed that for alloys with up to 9 mass%Al, without eutectoid for-

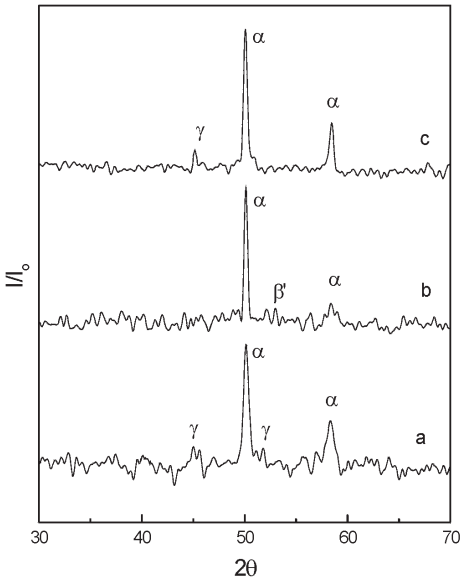

Fig. 7 X-ray diffraction patterns for Cu–19 at.%Al alloy: a – annealed; b – quenched from 850°C; c – quenched from 450°C after quenching from 850°C

mation, the height of this peak is increased with the increasing aluminum content. They attributed this peak to partial ordering assisted by diffusion of vacancies resulting from quenching from 450°C. The presence of the gamma phase in the alloys here studied seems to change this situation and the second exothermic peak, which is not observed for the Cu–17 at.%Al alloy, is now increased with the increase of the Al content. The height and extension of this second exothermic peak in Fig. 6c seem to indicate that reordering the alloy is taking place partially at 170 and mainly at 270°C, together with ordering the β' martensitic phase, i.e., the α_2 ordering process takes place in two stages.

In order to analyze the influence of the heating rate on β_1-phase decomposition a DSC curve at 30°C min^{-1} was obtained for Cu–21 at.%Al alloy quenched from 850°C before heating. From Fig. 6d it is possible to observe that the peak correspondent to the reverse martensitic transformation $\beta'_1 \rightarrow \beta_1$ and the decomposition $\beta_1 \rightarrow (\alpha+\gamma_1)$ from part of the β_1 phase is better defined. The peak at 535°C, due to the β_1 transition decreases and now it is possible to observe an exothermic peak at about 550°C. These effects may be related to the $\beta_1 \rightarrow (\alpha+\gamma_1)$ decomposition leading to the formation of the γ_1 phase (Al_4Cu_9) from the β_1 phase, at 400°C and the precipitation of the copper-rich solid solution α phase, at 550°C [7]. These results indicate that the $\beta_1 \rightarrow (\alpha+\gamma_1)$ decomposition is the dominant reaction, unlikely that observed for Cu–Al alloys near the eutectoid composition [7].

Figure 7 shows the X-ray diffraction patterns for Cu–19 at%Al alloy after annealing and after quenching. It is possible to observe the presence of the diffraction lines corresponding to the α and γ_1 phases, after annealing (Fig. 7a). After quenching, one can see the diffraction lines corresponding to the β' martensitic phase, with the lines for the α phase (Fig. 7b). The absence of the β' martensitic phase for temperatures higher than 400°C in samples quenched before heating, proposed to explain the results in curves b and c of Fig. 6 is confirmed by the diffraction pattern shown in Fig. 7c. In this figure, it is possible to observe only the diffraction lines corresponding to the α and γ_1 phases.

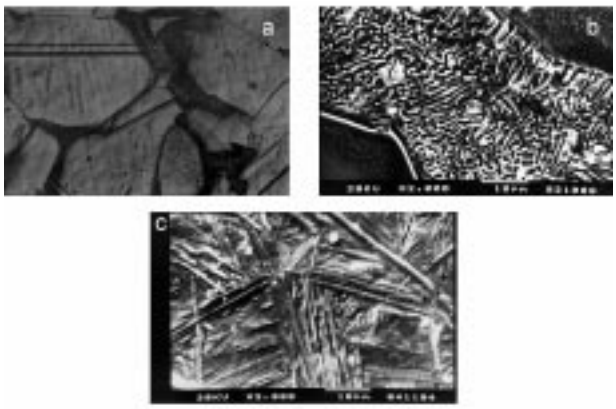

Fig. 8 Cu–19 at.%Al alloy: a – annealed (OM 150×); b – annealed (SEM); c – quenched from 850°C (SEM)

The microstructures identified by X-ray diffraction patterns are shown in Fig. 8 for Cu–19 at.%Al alloy after annealing and after quenching. It is possible to observe the structure characteristic of the α phase and the $(\alpha+\gamma_1)$ complex phase for the annealed sample (Figs 8a and 8b). Figure 8b shows the pearlitic microstructure and Fig. 8c the martensitic microstructure.

Conclusions

The presence of the γ_1 phase (Al_4Cu_9), clearly detected for the Cu–19 at.%Al alloy, caused the α_2 phase disordering process to occur in two stages, the first in the range from 100 to 200°C and the second from 250 to 350°C. The dissolution of α_2 precipitates seems to decrease with the increase in the Al concentration, in opposition to what was observed for alloys with up to 19.5 at%Al. This result is interpreted considering that the fraction of the α-matrix phase in the alloys exceeding the solubility limit of α-Cu–Al is decreased with the increase of the Al content, leading to a decrease in the dissolution of α_2 precipitates in the matrix.

The thermal response for the α_2 precipitates dissolution process is influenced by the heating/cooling ratio. A more reversible thermal response is obtained for small heating/cooling ratios, given a better defined peak. The presence of the endothermic peak corresponding to the $\beta_1 \rightarrow \beta$ transformation depends on an incomplete $(Cu)\text{-}\alpha+\beta \rightarrow (Cu)\text{-}\alpha+(\alpha+\gamma_1)$ decomposition reaction, which retains a small fraction of the martensitic phase. Therefore, for cooling rate in which the martensitic phase is not retained, e.g. 1°C min^{-1}, this endothermic peak is not observed. An increase in the heating rate from 20 to 30°C min^{-1} showed that the $\beta_1 \rightarrow (\alpha+\gamma_1)$ decomposition is the dominant reaction for alloys containing 19 and 21 at.%Al.

* * *

The authors thank FAPESP and CNPq for financial support.

References

1 G. Roulin and P. Duval, Scripta Mat., 37 (1997) 45.
2 G. Roulin, P. Duval and N. Le Guiner, Scripta Mat., 37 (1997) 253.
3 J. L. Murray, Int. Met. Rev., 30 (1985) 211.
4 D. R. F. West and D. L. J. Thomas, Inst. Met., 83 (1954–55) 505.
5 W. Gaudig and H. Warlimont, Acta Met., 26 (1978) 709.
6 J. Kwarciak, J. Thermal Anal., 31 (1986) 559.
7 J. Kwarciak, Z. Bojarski and H. Morawiec, J. Mat. Sci., 21 (1986) 788.
8 T. B. Massalski, Ed., Binary Alloy Phase Diagram, Vol. 1, 2nd Ed., ASM International, Ohio, USA 1992, p. 141.
9 W. Gaudig and H. Warlimont, Z. Metallk., 60 (1969) 488.
10 J. M. Popplewell and J. Crane, Met. Trans., 2 (1971) 3411.